

# Normalized Weighting Schemes for Image Interpolation Algorithms

Olivier Rukundo

Department of Clinical Sciences, Clinical Physiology, Lund University, Lund, Sweden  
[orukundo@gmail.com](mailto:orukundo@gmail.com)

**Abstract** – This work introduces four weighting schemes based on geometric shapes for image interpolation purposes. Geometric shapes of interests include the circle and triangle. The quantity used to express the extent of each shape is the normalized area. In the first scheme – the minimum diameter (MD) of a tetragon is used. In the second – the hypotenuse radius (HR) is used. In the third – the virtual pixel length-based height for the area of the triangle (AT) is used. In the fourth scheme – the virtual pixel length for hypotenuse-based radius for the area of the circle (AC) is used. Objective assessments demonstrated that, at a higher scaling ratio, the AC scored highest at 60% among new schemes presented. Subjective assessments demonstrated that the quality of images interpolated by the AC algorithm was superior or comparable to that of images interpolated by MD, HR, AT and selected traditional algorithms.

**Keywords** — circle; tetragon; normalization; hypotenuse; interpolation; triangle

## 1. INTRODUCTION

Commonly used normalization methods are based on interval arithmetic and fuzzy arithmetic [1]. Usually, normalization means rescaling variables, on the range between zero and one [2]. While this meaning holds in this work, it can vary from problem to problem in other works [3],[4]. Here, the news is normalization of areas, whose sum exceeds a unit square size, especially areas based on the Pythagorean theorem equation. In mathematics, the Pythagorean theorem is a fundamental relation in Euclidean geometry among the three sides of a right triangle [5]. Here, it can be written as equation Eq.1 or Eq.2 relating the lengths of the sides  $a$ ,  $b$ , and  $c$ , of a right-angled triangle [5]. The Pythagorean equation has been widely used in many computer sciences and engineering techniques, including in [6], [7], but, with very few times for image interpolation purposes [8]. In mathematics, interpolation is an estimation method used to construct a new data value within the range of a set of known data [9]. It is widely and routinely used in digital zooming [10]. Digital zoom is one of image processing techniques used to get a closer view of image objects, but it produces more visual artefacts than optical zooming. One of its advantages is that it does not require the mechanical device of lens elements such as the one used in optical zoom [10]. Artefact-free digital image zooming remains very challenging to achieve due to

the inaccuracy of interpolation algorithms and digital format requirement. There are currently many approaches to interpolation problems, particularly techniques developed to efficiently reduce visual artefacts in interpolated images or contribute other image processing tasks [10-12], [22-43]. A recent work, presented in [13], examined the origin of image pixels and divided image interpolation approaches into two major categories of non-extra-pixel and extra-pixel interpolation. Unlike, the extra-pixel approach, the non-extra pixel approach only depends on original or source image pixels [13]. It is important to note that, unlike the non-extra pixel, the extra-pixel approach category attracted many researchers, until now. In the extra pixel category, there are adaptive and non-adaptive interpolation techniques [8], [14], [15]. Also, among adaptive and non-adaptive, some techniques depend on traditional techniques, such as bilinear, to achieve improved outcomes relevant to the targeted problem or application of interest [14-21]. Here, the contribution is the introduction of new weighting schemes for image interpolation algorithms. The rest of the paper includes the Pythagorean theorem and normalization, normalized and virtual pixel length-based weighting schemes, experimental and conclusion parts.

## 2. PYTHAGOREAN THEOREM AND NORMALIZATION

Named after the Greek mathematician Pythagoras, the theorem can be reduced to Eq.1 and Eq.2.

$$a^2 + b^2 = c^2 \quad (1)$$

$$a^2 \leq c^2 - b^2 \quad (2)$$

where  $a$  and  $b$  are called legs or catheti of the right triangle and  $c$  is called hypotenuse, as shown in Figure 1.

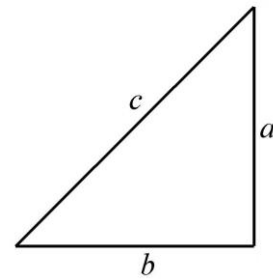


Figure 1:  $c$  = hypotenuse,  $b$  and  $a$  = legs (or base and height)

Now, referring to [2], the normalization of an  $n$ -tuple of general weights to the corresponding  $n$ -tuple of normalization weights is described by the real-vector-valued function

$n:W_n \rightarrow S_n$  defined for all  $(w_1, \dots, w_n) \in W_n$  in the following way shown in Eq. 3.

$$n(w_1, \dots, w_n) := \left( \frac{w_1}{\sum_{i=1}^n w_i}, \dots, \frac{w_n}{\sum_{i=1}^n w_i} \right) \quad (3)$$

Note that the normalization given by Eq. 3 provides weights whose sum is equal to one.

### 3. NORMALIZED WEIGHTING SCHEMES

**A. Tetragonal area:** A tetragon is another name for a quadrilateral [44],[45]. It has properties such as having four sides or edges, four vertices or corners, and interior angles that add to 360 degrees [44]. Figure 2 shows that the unit square (P1, P2, P3, P4) is composed of four tetragons with areas depending on the x-y coordinates of P. Such areas, for example  $W_3 = (x_2 - x) \times (y - y_1)$ , are used as pixel weights and P value is obtained using Eq. (4).

$$P_{(x,y)} = \sum_{i=1}^4 (W_i \times P_i) \quad (4)$$

Here, it is important to note that the sum of all weights must be equal to one.

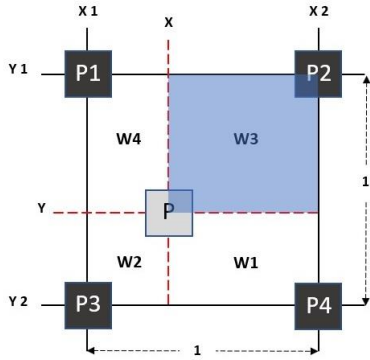


Figure 2: Tetragon

However, given that 4 tetragons areas sum up to 1, in this case, there is no need for normalization of the area or weight.

**B. Minimum side-based diameter :** Here, the minimum side length of any tetragons (if it is in the unit square), is used as the diameter of a circle, as shown in Figure 3. When the diameter is known, the area is calculated using Eq. 5.

$$A = \frac{\pi}{4} \times \text{diameter}^2 \quad (5)$$

Here, it is important to note that this Eq.5-based area replaces the pixel weights, in Eq. 4. However, given that the four circular areas do not sum up to one, in this case, there is need for weight normalization, using Eq.3.

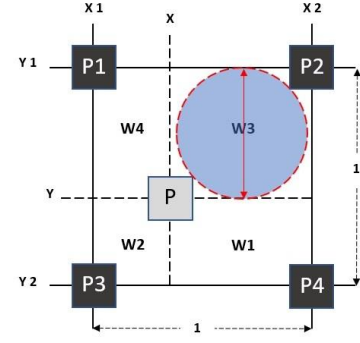


Figure 3: Minimum side-based diameter

**C. Hypotenuse-based radius:** In the right-angled triangle, the hypotenuse is the longest side of the triangle. As shown in Figure 4, the hypotenuse is used as the radius of the circle. When the radius is known, the area of the circle is calculated using Eq. (6).

$$A = \pi \times \text{radius}^2 \quad (6)$$

Also, here, it is important to note that this Eq.6-based area replaces the pixel weights, in Eq. 4. However, given that the four circular areas do not sum up to one, there is need for weight normalization, using Eq.3.

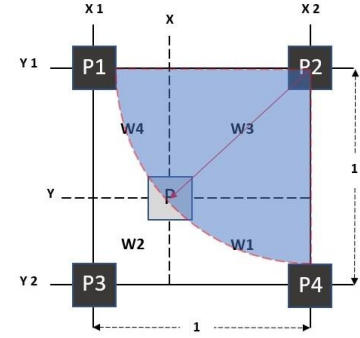


Figure 4: Hypotenuse-based radius

**D. Preliminary experiments:** Figure 5 shows the preliminary interpolation outcomes from the traditional bilinear or tetragon-based algorithm (TB), minimum side-based diameter algorithm (MD), and hypotenuse -based radius algorithm (HR). As can be seen, the basic structures and features, in the red square test image, are relatively recovered after image interpolation, using the scaling ratio = 4.



Figure 5: TB (top-right), MD (bottom-left), HR (bottom-right)

#### 4. VIRTUAL PIXEL LENGTH-BASED NORMALIZED WEIGHTING SCHEMES

It is important to note that, in this part, the virtual pixel length is equivalent to the grayscale pixel value.

*A. Virtual pixel length-based height:* In this scheme, we refer to Figure 6, where the virtual pixel length (A) is used as the height of the triangle. Now, with the hypotenuse (B) as the base of the triangle, the area of the triangle can be calculated using Eq. 7.

$$A = \frac{1}{2} \times \text{Base} \times \text{Height} \quad (7)$$

It is important to note that the Eq.6-based area replaces the pixel weights, in Eq. 4. And, given that the four triangular areas do not sum up to one, there is need for weight normalization, using Eq.3.

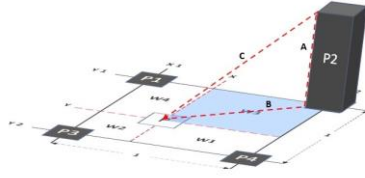


Figure 6: Virtual pixel length-based height

*B. Virtual pixel length for hypotenuse-based radius:* Figure 7 shows the virtual pixel length (A), the base (B), and the hypotenuse (C). In this case, the hypotenuse (C) is used as the radius to find the area of a circle, using Eq. (6).

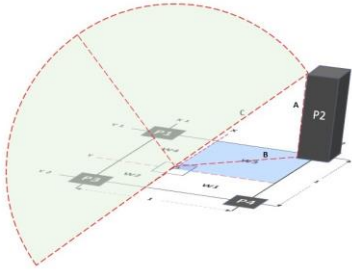


Figure 7: Virtual pixel length for hypotenuse-based radius

In Figure 7 case, the Eq.6-based area replaces the pixel weights, in Eq. 4. And, given that the four circular areas do not sum up to one, there is need for weight normalization, using Eq.3. Apart from that, it is important to note that this is inspired by one of the works presented in [36], in which the Pythagorean theorem equation was preliminary used, to tackle the image interpolation algorithmic efficiency, as the main concern.

#### 5. EXPERIMENTS

In this part, the popular datasets, and image quality assessment (IQA) metrics are described and defined, respectively. Image interpolation algorithms to be evaluated include the traditional nearest neighbor (TN), bicubic (TC), bilinear (TB), normalized minimum side diameter-based (MD), normalized hypotenuse radius-based (HR), normalized

virtual pixel length-based height for the area of the triangle (AT), and normalized virtual pixel length for hypotenuse-based radius for the area of the circle (AC). The mentioned interpolation algorithms were manually implemented in MATLAB software (R2020a). Objective and subjective image quality assessments are also presented and discussed.

*A. Dataset:* Here, the image dataset used contained 210 Textures, Aerials, Miscellaneous, and Sequences images downloaded from the USC-SIPI Database [46]. These images were resized to  $512 \times 512$ ,  $256 \times 256$ , and  $128 \times 128$ , and converted to 8bits, using R2020a MATLAB software. The resized versions are accessible via [GitHub.com/orukundo](https://github.com/orukundo) [47] – and each size category contains 210 different images.

*B. IQA Metrics:* Here, only full reference IQA metrics were chosen to quantify the closeness or similarity of interpolated images against their corresponding pristine images [15]. Those chosen are the mean-squared error (MSE), structural similarity index (SSIM), and peak signal to noise ratio (PSNR). Given that these metrics are widely used, more details can be found in the literature and software, therefore not included in this part. It is important to note that, MATLAB's TIC and TOC functions were used to measure the speed of different interpolation algorithms, at different scaling ratios, in terms of the elapsed time in seconds. Also, note that, here, the average means the average score, or performance achieved by each mentioned algorithm on 210 test images.

*C. Objective image interpolation quality assessment:* As can be seen, in Figure 8, the TN is the fastest of all algorithms, mentioned, because, in each scaling ratio case, it used the smallest average time, among other methods mentioned. The elapsed time showed that TB is faster than MD, HR, AT, and AC. This can be explained by the new weighting schemes which included more computations thus increasing their MATLAB lines reading time. It is important to note that the software built-in versions (TN, TB, TC) normally perform better than the manually implemented versions. Note that, in each scaling ratio case, TC produced the best results among other methods mentioned. In other words, TC scored highest at 100% among all other methods mentioned (considering that the maximum number of times each method could score highest at 100% was 3 when the scaling ratio was equal to 2 and 4).



Figure 8: Average time (in seconds)

In Figure 9, the average results of each interpolation algorithm in terms of MSE are presented. As can be seen, the

MSE errors of each method could be generalized, even if there were exceptions with built-in functions based methods such as TN, TB, and TC. For example, the TN exception could be based on the type of images used in the experiment, since it is generally perform badly with only interpolating grain texture images [19].

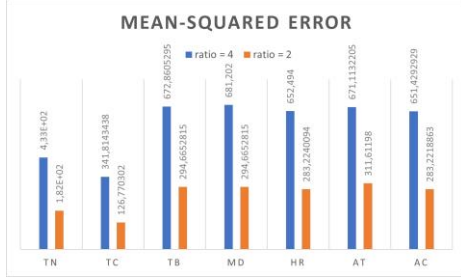


Figure 9: Average MSE

Now, referring to the MSE metric - when scaling ratio = 2, AC achieved better results than MD, AT, HR. And, when scaling ratio = 4, AC again achieved better results than MD, AT, HR.

In Figure 10, referring to the SSIM metric - when scaling ratio = 2, AT achieved better results than MD, AC, HR. And, when scaling ratio = 4, MD achieved better results than AC, AT, HR.

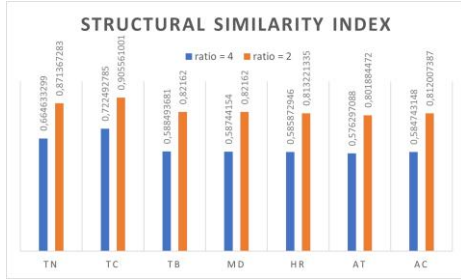


Figure 10: Average SSIM

In Figure 11, referring to the PSNR metric - when scaling ratio = 2, HR achieved better results than MD, AC, AT. And, when scaling ratio = 4, AC achieved better results than MD, AT, HR.

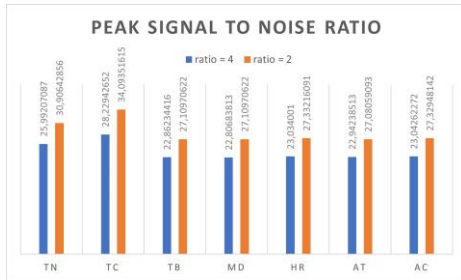


Figure 11: Average PSNR

To simply the understanding of results presented in Figure 9, Figure 10 and Figure 11, simplified representation of results is given in Table 1 and Table 2. In these tables the maximum number of times to score highest is equal three because there are three IQA metrics, namely: MSE, SSIM and PSNR. Here, a method that outperforms others, in terms of the above three metrics, will score highest at 100%.

Table 1: Simplified representation of results (traditional vs new schemes)

	TN	TB	TC	MD	HR	AT	AC
2x	0	0	3	0	0	0	0
4x	0	0	3	0	0	0	0

Table 2: Simplified representation of results (new schemes)

	MD	HR	AT	AC
2x	0	1	1	1
4x	1	0	0	2

*D. Subjective image interpolation quality assessment:* From left to right - on the first row of Figure 12 (Boat), Figure 13 (Man), and Figure 14 (Clock), there are TN, TC and TB test images. On the second row, there are MD, HR, AT and AC test images. In Figure 12, edges are jagged while others are not, especially vertical and horizontal edges of the TN image. Here, the TN algorithm did not produce blurred edges. In the TC image, the oblique, vertical and horizontal edges look blurred to some extent but not jagged. In the TB image, regardless of the edge direction, the edges are blurred but not jagged.



Figure 12: Boat test image

In the MD image, edges are slightly blurred and jagged. In the HR image, the edges are blurred and slightly jagged. In the AT image, the edges are blurred and jagged, especially at the oblique edges. In the AC image, the edges are slightly blurred and slightly jagged, especially at the oblique edges, which makes AC the best among new schemes and slightly superior or comparable to TC in terms of the visual quality. This situation is quasi-repeated in Figure 13 and Figure 14, which involved different images. In some of the presented figures' cases, edges are clearly defined, which may lead to different conclusions, since the performance of any image interpolation algorithm remains dependent on the type of input image.



Figure 13: Man test image



Note that the quality of images presented here is affected, to some extent, by compression artefacts and viewing directly from the paper format.



Figure 14: Clock test image

## 6. CONCLUSION

Four weighting schemes were presented in this work, and their effects were experimentally demonstrated. In our experiments, specifically in the first part aimed at comparing all methods (i.e., traditional and new scheme methods), for the scaling ratio = 2 and 4, objective image interpolation quality assessment showed that the TC method scored highest at 100% among all other methods, mentioned. In the second part of our experimental demonstrations, that aimed at comparing new schemes, for the scaling ratio = 2, objective image interpolation quality assessment showed that the MR scored highest at 0%, HR scored highest at 30%, AT scored highest at 30%, AC scored highest at 30%. In the same part, for the scaling ratio = 4, objective image interpolation quality assessment showed that the MR scored highest at 30%, HR scored highest at 0%, AT scored highest at 0%, AC scored highest at 60%. Subjective image quality assessment showed that the overall performance of the AC algorithm was superior or comparable to TN, TB, TC, MD, HR, and AT. Note that, in digital image processing and analysis, there exist no method that best works for all kinds of images. It is important to note that many medical/biomedical image processing and analysis software still rely on the TN, TB and TC. Also, it is important to note that the TN remained the fastest method among all methods mentioned in terms of average time taken by each method to process an image. Future efforts may focus on developing intelligent weight assignment schemes.

## ACKNOWLEDGEMENT

This work was done at Lund University. The author would like to thank reviewers and editors for their helpful comments.

## CONFLICT OF INTEREST

The author declares no conflict of interest.

## REFERENCES

- [1] Y.M., Wang, T.M.S., Elhag, On the normalization of interval and fuzzy weights, *Fuzzy Sets and Systems*, 157, 2006, pp. 2456 – 2471
- [2] O., Pavlacka, On various approaches to normalization of interval and fuzzy weights, *Fuzzy Sets and Systems*, 243, 2014, pp. 110 – 130
- [3] R.C., González, R.E., Woods, *Digital Image Processing*, Prentice Hall., 2007, p. 85
- [4] F., Daniel, K., Julia, *A Student's Guide to the Mathematics of Astronomy*, Cambridge University Press, 2013, p. 35
- [5] J.D., Sally, P., Sally, Chapter 3: Pythagorean triples. *Roots to research: a vertical development of mathematical problems*. American Mathematical Society Bookstore. 2007, page 63
- [6] A.S., Sadiq, T.Z., Almomhammad, et al., An Energy-Efficient Cross-Layer approach for cloud wireless green communications, *2017 Second International Conference on Fog and Mobile Edge Computing (FMEC)*, Valencia, 2017, pp. 230-234
- [7] H.G., Fu, L., Yang, C.C., Zhou, A computer-aided geometric approach to inverse kinematics, *Journal of Robotic Systems*, 15(3), 1998, pp. 131-143
- [8] O., Rukundo, *Optimal Methods Research on Grayscale Image Interpolation*, CNKI, TP391.41, 2012
- [9] W.F., Sheppard, *Interpolation*, In Chisholm, Hugh (ed.). *Encyclopædia Britannica*. 14 (11th ed.), Cambridge University Press., 1911, pp. 706–710
- [10] O., Rukundo, *Evaluation of Rounding Functions in Nearest-Neighbour Interpolation*, arXiv:2003.06885, 2020, p. 1-8
- [11] Tian, Q. C., Wen, H., et al.: A fast edge-directed interpolation algorithm. In: Huang, T.W., Zeng, Z.G., Li, C.D., Lueng, C.S. (eds.) *International Conference on Neural Information Processing*, LNCS, vol. 7665, 2012, pp. 398–405
- [12] S., Khan, D.H., Lee, et al., "Image Interpolation via Gradient Correlation-Based Edge Direction Estimation", *Scientific Programming*, vol. 2020, Article ID 5763837, 12 pages, 2020
- [13] O., Rukundo, Non-extra Pixel Interpolation, *International Journal of Image and Graphics*, Vol. 20, Issue 4, 2050031, 2020, p. 1-14
- [14] O., Rukundo, S., Schmidt, Effects of Rescaling Bilinear Interpolant on Image Interpolation Quality, *Proc. SPIE 10817, Optoelectronic Imaging and Multimedia Technology V*, 1081715, 2018
- [15] O., Rukundo, S., Schmidt, Extrapolation for Image Interpolation, *Proc. SPIE 10817, Optoelectronic Imaging and Multimedia Technology V*, 108171F, 2018
- [16] L., Zhang, X., Wu., An edge-guided image interpolation algorithm via directional filtering and data fusion. *IEEE Transactions on Image Processing*, 15(8), 2006, pp. 2226–2238
- [17] X., Li, M. T., Orchard : New edge-directed interpolation. *IEEE Transactions on Image Processing*, 10(10), 2001, pp. 1521–1527
- [18] O., Rukundo, M.H. Huang and H.Q. Cao, Optimization of Bilinear Interpolation Based on Ant Colony Algorithm", *Proc. 2nd Int. Conf. Electrical and Electronics Engineering*, Macao, Dec.1-2, 2011. pp. 571-580
- [19] O., Rukundo and H.Q. Cao, *Advances on Image Interpolation Based on Ant Colony Algorithm*, SpringerPlus, 5:403, 2016
- [20] O., Rukundo and H.Q., Cao, Nearest Neighbor Value Interpolation, *International Journal of Advanced Computer Science and Applications (IJACSA)*, 3(4), 25 - 30, May 2012
- [21] O., Rukundo, Effects of Improved-Floor Function on the Accuracy of Bilinear Interpolation Algorithm, *Computer and Information Science*, Vol.8, No.4, 2015, pp.1–25
- [22] Z.Z., Huang, L.C., Cao, Bicubic interpolation and extrapolation iteration method for high resolution digital holographic reconstruction, *Optics and Lasers in Engineering*, Volume 130, 2020, 106090
- [23] Y.H., Lee, N.A., Yu, C.Y., Tsai, an image-upscaling engine for 1080p to 4k using gradient-based interpolation, *International Journal of Electronics*, 107:9,2020, pp.1386-1405
- [24] G., Xu, R., Ling, L., Deng, Q., Wu, W., Ma, Image interpolation via gaussian-sinc interpolators with partition of unity, *Computers, Materials & Continua*, vol. 62, no.1, 2020, pp. 309–319
- [25] Zulkifli NAB, Karim SAA, Shafie AB, Sarfraz M, Ghaffar A, Nisar KS. Image Interpolation Using a Rational Bi-Cubic Ball. *Mathematics*. 2019; 7(11):1045
- [26] O., Rukundo, K.N. Wu and H.Q. Cao., Image Interpolation Based on The Pixel Value Corresponding to The Smallest Absolute Difference, in *Proc. 4th Int. Workshop. on Advanced Computational Intelligence*, Wuhan, 2011, pp. 434-437
- [27] O., Rukundo, B.T., Maharaj, Optimization of Image Interpolation based on Nearest Neighbour Algorithm. *9th Int. Conf. on Computer Vision Theory and Applications (VISAPP 2014)*, Lisbon, 2014, pp. 641–647

- [28] O., Rukundo, M., Pedersen, Ø., Hovde, Advanced Image Enhancement Method for Distant Vessels and Structures in Capsule Endoscopy, Computational and Mathematical Methods in Medicine, vol. 2017, Article ID 9813165, 13 pages, 2017
- [29] O., Rukundo, S., Schmidt, Aliasing Artefact Index for Image Interpolation Quality Assessment, Proc. SPIE 10817, Optoelectronic Imaging and Multimedia Technology V, 108171E, 2018
- [30] O., Rukundo, Half-Unit Weighted Bilinear Algorithm for Image Contrast Enhancement in Capsule Endoscopy, Proc. SPIE 10615, Ninth International Conference on Graphic and Image Processing (ICGIP 2017), 106152Q, 2018
- [31] O., Rukundo, E.S., Schmidt, O.T.V., Ramm, Software Implementation of Optimized Bicubic Interpolated Scan Conversion in Echocardiography, arXiv:2005.11269, 2020, p. 1-10
- [32] O., Rukundo, Effects of Empty Bins on Image Upscaling in Capsule Endoscopy, Proc. SPIE 10420, Ninth International Conference on Digital Image Processing (ICDIP 2017), 104202P, July 21, 2017
- [33] M., Rucka, E., Wojtczak, M., Zielińska, Interpolation methods in GPR tomographic imaging of linear and volume anomalies for cultural heritage diagnostics, Measurement, Volume 154, 2020, 107494
- [34] Y.Q., Chen, W.J., Sun, L.Y., Li, et al., An efficient general data hiding scheme based on image interpolation, Journal of Information Security and Applications, Volume 54, 2020, 102584
- [35] X.H., Wang, X.Y., Jia, W. Zhou, et al., Correction for color artifacts using the RGB intersection and the weighted bilinear interpolation, Appl. Opt. 58, 2019, pp. 8083-8091
- [36] F.S., Hassan, A., Gutub, Efficient reversible data hiding multimedia technique based on smart image interpolation, Multimedia Tools and Applications (2020) 79:30087–30109
- [37] C.J., Jiang, H.T., Li, S.B., Zhou, et al., Image interpolation model based on packet losing network, Multimedia Tools and Applications (2020) 79:25785–25800
- [38] De Feis I, Masiello G, Cersosimo A. Optimal Interpolation for Infrared Products from Hyperspectral Satellite Imagers and Sounders. Sensors. 2020; 20(8): 2352
- [39] T., Moraes, P., Amorim, J., Vicente Da Silva, H., Pedrini, Medical image interpolation based on 3D Lanczos filtering, Computer Methods in Biomechanics and Biomedical Engineering: Imaging & Visualization, 8:3, 2020, 294-300
- [40] W.L., Huang, J.X., Liu, Robust Seismic Image Interpolation with Mathematical Morphological Constraint, IEEE Transactions on Image Processing, Vol.29, 2020, pp. 819-829
- [41] G., Song, C., Qin, K., Zhang, X., Yao, F., Bao, Y., Zhang, "Adaptive Interpolation Scheme for Image Magnification Based on Local Fractal Analysis," in IEEE Access, vol. 8, 2020, pp. 34326-34338
- [42] M., Murad, M., Bilal, A., Jalil, et al., Efficient Reconstruction Technique for Multi-Slice CS-MRI Using Novel Interpolation and 2D Sampling Scheme, in IEEE Access, vol. 8, 2020, pp. 117452-117466
- [43] J., Ji, B., Zhong and K.K., Ma, Image Interpolation Using Multi-Scale Attention-Aware Inception Network, in IEEE Transactions on Image Processing, vol. 29, 2020, pp. 9413-9428
- [44] Quadrilaterals, <<https://www.mathsisfun.com/quadrilaterals.html>>, Accessed: 2020-11-01
- [45] List of Geometry and Trigonometry Symbols, Math Vault, <<https://mathvault.ca/hub/higher-math/math-symbols/geometry-trigonometry-symbols/>>, Accessed: 2020-11-01
- [46] USC-SIPI Image Database: <http://sipi.usc.edu/database/database.php>, 2020-11-08
- [47] Modified-USC-SIPI-Image-Database: <https://github.com/orukundo/Modified-USC-SIPI-Image-Database>, 2020-11-08